HHS Public Access

Author manuscript

Immunol Cell Biol. Author manuscript; available in PMC 2014 February 24.

Published in final edited form as:

Immunol Cell Biol. 2013 May ; 91(5): 368–376. doi:10.1038/icb.2013.11.

Targeted Disruption of MCPIP1/Zc3h12a Results in Fatal Inflammatory Disease

Ruidong Miao[1,6,*], **Shengping Huang**[1,*], **Zhou Zhou**[2,*], **Tim Quinn**[1], **Ben Van Treek**[1], **Tehreem Nayyar**[1], **Daniel Dim**[3], **Zhisheng Jiang**[4], **Christopher J. Papasian**[1], **Y. Eugene Chen**[2], **Gang Liu**[5], and **Mingui Fu**[1,7]

[1]Department of Basic Medical Science, School of Medicine, University of Missouri Kansas City, Kansas City, MO 64108

[2]Cardiovascular Center, Department of Internal Medicine, University of Michigan Medical Center, Ann Arbor, MI 48109

[3]Department of Pathology, University of Missouri Kansas City, Kansas City, MO 64108

[4]Institute of Cardiovascular Disease, School of Medicine, University of South China, Hengyang City, Hunan Province, P.R.China, 421001

[5]Division of Pulmonary, Allergy & Critical Care Medicine, University of Alabama at Birmingham, Birmingham, AL 35294

[6]School of Life Sciences, Lanzhou University, Lanzhou 730000, PR China

Abstract

Previous studies using MCPIP1/Zc3h12a-deficient mice suggest that MCPIP1 is an important regulator of inflammation and immune homeostasis. However, the characterization of the immunological phenotype of MCPIP1-deficient mice has not been detailed. In this study, we performed evaluation through histological, flow cytometric, ELISA and real-time PCR analysis and found that targeted disruption of MCPIP1 gene leads to fatal, highly aggressive, and widespread immune-related lesions. In addition to previously observed growth retardation, splenomegaly, lymphoadenopathy, severe anemia and premature death, MCPIP1-deficient mice showed disorganization of lymphoid organs, including spleen, lymph nodes and thymus, and massive infiltration of lymphocytes, macrophages and neutrophils into many other non-lymphoid organs, primarily in lungs and liver. Flow cytometric analysis found significant increase in activated and differentiated T cells in peripheral blood and spleen of MCPIP1-deficient mice. Moreover, heightened production of inflammatory cytokines from activated macrophages and T cells were observed in MCPIP1-deficient mice. Interestingly, treatment of MCPIP1-deficient mice with antibiotics resulted in significant improvement of life-span and a decrease in inflammatory

[7]Correspondence to Mingui Fu, PhD, Department of Basic Medical Science, School of Medicine, University of Missouri Kansas City. 2411 Holmes Street, Kansas City, MO 64108. Phone: 816-235-2193 Fax: 816-235-6444 fum@umkc.edu.

*R.M., S. H. and Z.Z. equally contributed to this work.

Conflict of Interest

The authors have no financial conflicts of interests.

syndrome. Taken together, these results suggest a prominent role for MCPIP1 in the control of inflammation and immune homeostasis.

Keywords

MCPIP1; autoimmune disease; inflammation; cytokine; lymphocyte

Introduction

As the immune system is continuously bombarded with foreign antigens, complex regulatory mechanisms interact to maintain immune homeostasis. Specifically, the inflammatory and immune responses must be sufficient to eliminate invading antigens, but the inflammatory response should not be sustained after the threat has been eliminated and, ideally, the invader should be eliminated without substantial collateral damage to surrounding tissues [1,2]. The molecular mechanisms contributing to maintenance of immune homeostasis are not fully understood. We and others recently identified a novel member of CCCH-zinc finger protein family, designated as MCPIP1 (also known as Zc3h12a), which is 65.8 kDa protein encoded by the immediate-early response gene, Zc3h12a [3–7]. This gene has been mapped to chromosome 4 in mouse, and the equivalent gene in human, ZC3H12A, has been mapped to chromosome 1p34.3. In adult mouse, MCPIP1 mRNA is highly expressed in lung, intestine, colon, lymph node, spleen, and thymus. MCPIP1 mRNA is expressed at lower levels in stomach, bladder, adipose tissue, and the aorta, and is essentially absent in brain, kidney, liver, heart and skeletal muscle[8]. Several members of the MCPIP1 family, including MCPIP1/Zc3h12a, Zc3h12b, Zc3h12c and Zc3h12d, were previously reported to contribute to negative regulation of lipopolysaccharide (LPS)-induced macrophage activation[4]. These initial findings were further confirmed by observations in MCPIP1-deficient mice [8,9]. MCPIP1-deficient mice develop normally *in utero*. However, with age, they begin to suffer from spontaneous inflammatory diseases characterized by multi-organ inflammation, splenomegaly, heightened inflammatory cytokine production and premature death [8,9]. MCPIP1-deficient cells are hyper-responsive to Toll-like receptor (TLR) signaling, and MCPIP1-deficient mice are hypersensitive to septic shock[10]. Furthermore, we and others have recently shown that MCPIP1 is a multifunctional protein that actively participates in several distinct signaling pathways. For example, MCPIP1 down-regulates LPS-induced inflammatory responses by acting as an RNase[9, 11]; MCPIP1 inhibits JNK and NF-κB signaling by interfering with the ubiquitination of upstream signaling molecules, such as TRAFs[8]. These results collectively suggest that MCPIP1 is a novel anti-inflammatory protein that negatively regulates both innate and adaptive immunity, and that its selective expression in lymphoid and inflamed tissues suppresses hyper-responsiveness, thereby contributing to the maintenance of immune homeostasis.

The goal of the current study was to further characterize the phenotypes of MCPIP1-deficient mice through histological, flow cytometric, ELISA and real-time PCR analysis. We found that targeted disruption of MCPIP1 gene resulted in fatal disseminated inflammation, which was characterized by disrupted architecture of primary and secondary lymphoid organs, leukocytic infiltration of lungs and liver, activation of T cells and B cells,

and enhanced levels of both macrophage and T cell derived cytokines. These results demonstrated a prominent role for MCPIP1 in control of inflammation and immune homeostasis.

Results

Primary and secondary lymphatic tissues of MCPIP1-deficient mice exhibit architectural disorganization

Despite the striking phenotypic changes reported for MCPIP1$^{-/-}$ mice in our previous study[8], the detailed pathogenesis of these alterations was not fully analyzed. Consquently, in the current study, we further characterized the changes occurring in the major organs and tissues, including thymus, spleen, lymph nodes, lungs, liver, heart, aorta, kidney, skin, and intestine etc., from MCPIP1 deficient mice by histological, flow cytometric and real-time PCR analysis. The most strinking morphological changes were observed in spleen, lymph nodes and thymus of MCPIP1-deficient mice. As shown in Fig.1a, the architecture of the spleen, lymph nodes and thymus from both male and female MCPIP1-deficient mice at 8-weeks of age appeared disorganized. In the spleen, the white pulp appeared underdeveloped, whereas the red pulp had marked expansion, probably a result of extramedullary hematopoiesis. Such pathology disrupted normal splenic architecture. In lymph nodes of MCPIP1-deficient mice, normal follicular architecture of the cortex was missing, which was probably caused by underdevelopment. The paracortical areas were also disorganized. In the thymus, the cortex was essentially absent and the medulla was significantly expanded. To investigate the development of this architectural disruption with age, we futher observed the phenotype of MCPIP1-deficient mice at the ages of 2-days, 3-weeks and 6-weeks. As shown in Fig.1b–d, the gross size and histological morphology of spleens from MCPIP1$^{-/-}$mice at the age of 2-days were essentially normal compared with those from wild-type littermates. By 3 weeks of age, spleens from MCPIP1$^{-/-}$ mice were obviously larger than those from MCPIP1$^{+/+}$ littermates, and these differences became even more pronounced by 6-weeks of age. These results suggest that the architectural abnormalities observed in primary and secondary lymphatic tissues of MCPIP1-deficient mice progressed with age.

MCPIP1-deficient mice exhibit multi-organ inflammation

The gross architecture of the non-lymphoid organs from MCPIP1-deficient mice was essentially normal compared with that from wild-type littermates (at the age of 8-weeks). Microscopically however, multifocal and mixed inflammatory cell infiltration was observed in many of these organs, with the most severe changes occurring in the lungs and liver from MCPIP1-deficient mice (Fig.2 & Fig. S1). At 3-weeks of age leukocyte infiltration into the interstitial spaces of the lungs was observed in MCPIP1$^{-/-}$ mice, but not in MCPIP1$^{+/+}$ mice (Fig.2a). By 8-weeks of age, massive infiltration of leukocytes into the interstitial spaces of the lungs, marked thickening of the alveolar septa, and pulmonary edema were observed in MCPIP1$^{-/-}$ mice, but not in MCPIP1$^{+/+}$ mice. Large amounts of mucus also filled the terminal bronchioles and alveolar spaces of MCPIP1$^{-/-}$ mice by 8 weeks. In the liver, inflammatory cell infiltration in the portal triad area, with infiltrates most concentrated near the bile ducts, was observed in MCPIP1$^{-/-}$ mice, but not in MCPIP1$^{+/+}$ mice (Fig.2b). Mild to moderate inflammatory cell infiltration was also observed in intestines, and kidneys from

MCPIP1$^{-/-}$ mice. It was also noted that transmural thickening of the intestine also appeared in MCPIP1$^{-/-}$ mice. In the kidneys of MCPIP1$^{-/-}$mice, the glomeruli were larger, with a skewed matrix to nuclei ratio (Fig. S1). There was no microscopic evidence of bacterial invasion into these tissues. No significant inflammation was observed in other tissues of MCPIP1$^{-/-}$ mice, such as heart, aorta and skin, despite there was some minor inflammatory cell infiltration into adipose tissue surrounding the aorta (Fig. S1). Immunohistochemical staining demonstrated that most of the inflammatory cells in the lungs were B lymphocytes and macrophages, whereas in the liver, predominately neutrophils and macrophages (Fig. 2c).

MCPIP1-deficient mice exhibit increased immunoglobulin accumulation in multiple tissues

Previous report showed that MCPIP1/Zc3h12a null mice developed hyperimmunoglobulinemia of all immunoglobulin isotypes[9]. Anti-nuclear antibodies and anti-double-stranded-DNA antibodies were also detected in MCPIP1/Zc3h12a null mice[9]. In the current study, immunofluorescent staining revealed increased accumulation of IgM and IgG in multiple organs from MCPIP1$^{-/-}$ mice, including spleen, skin, lungs and aorta, but not in those from MCPIP1$^{+/+}$ mice (Fig.3). Interestingly, the accumulation of immune complex was not obvious in the kindey from MCPIP1$^{-/-}$ mice (Fig.3). Nevertheless, these results demonstrated that MCPIP1-deficient mice spontanously developed an autoimmune response.

Immune cell abnormalities in MCPIP1-deficient spleens

To further characterize the cellular components of the systemic inflammation in MCPIP1-deficient mice, we performed flow cytometry analysis of cell populations in the spleens of MCPIP1$^{-/-}$ and MCPIP1$^{+/+}$ mice. First, we analyzed nucleated spleen cells to determine the percentage of B cells, T cells, neutrophils and monocytes and found that the percentage of B cells in the spleen was dramatically decreased, the percentage of neutrophils was markedly increased, and the percentage of T cells was moderately decreased in MCPIP1$^{-/-}$ mice; monocytes remained essentially unchanged (Fig.4a). Interestingly, although B cells represented a relatively small percentage of nucleated cells in the spleens of MCPIP1$^{-/-}$ mice (approximately 7%), a surprisingly high proportion of these cells had differentiated into plasma cells (approximately 25%) (Fig.4a). To further explore lymphocyte activation within the spleen, we studied various T cell populations. Specifically, we compared the levels of activation of CD4^{+} and CD8^{+} cells from the spleens of MCPIP1$^{-/-}$ and MCPIP1$^{+/+}$ mice using the specific markers for activated T cells (CD62L), Th1 (IFN-γ), and Th2 (IL-4). As shown in Fig.4b&c, CD62L^{low} was significantly upregulated in both CD4^{+} and CD8^{+} cells from MCPIP1$^{-/-}$ mice compared to those from MCPIP1$^{+/+}$ mice, suggesting that T cells were automaticlly activated in MCPIP1$^{-/-}$ mice. Moreover, INFγ was also significantly upregulated in both CD4^{+} and CD8^{+} cells from MCPIP1$^{-/-}$ mice AND IL-4 was significantly elevated in CD4+ cells, but not in CD8+ cells of MCPIP1−/− mice (Fig.4c). These findings support that lymphocyte activation and differentiation was profoundly enhanced in spleens of MCPIP1$^{-/-}$ compared to that in MCPIP1$^{+/+}$ mice. In addition, the percentage of both CD4^{+} and CD8^{+} cells expressing IL-17 was significantly increased in MCPIP1$^{-/-}$ compared to MCPIP1$^{+/+}$ mice (Fig.4c). In view of the profound proinflammatory effects of IL-17, it is probable that enhanced expression of IL-17 in

MCPIP1$^{-/-}$ mice contributed to acute inflammatory changes observed within the spleens from these mice. Somewhat surprisingly, Foxp3 expressing cells were also more prominent in spleens from MCPIP1$^{-/-}$ mice, particularly among CD4^{+} cells (Fig.4b&c). Consequently, the profound inflammatory response in spleens of MCPIP1$^{-/-}$ mice could not be attributed to deficient numbers of T_{reg} cells.

MCPIP1-deficient mice exhibit increased protein and mRNA levels for markers of innate and adaptive immunity

To further delineate the molecular mechanisms underlying the fatal inflammation in MCPIP1$^{-/-}$ mice, we examined protein level of 23 proinflammatory cytokines, chemokines, and other markers of inflammation in serum of 2-month old mice (not all data are shown). As shown in Fig.5a, the pro-inflammatory cytokines from both innate cells (such as IL-1, IL-6, MCP-1 and TNFα) and adaptive immune cells (such as IL-2, IL-3, IL-4, IL-5, IL-12p40, IL-13, IL-17 and IFNγ) were all increased in the serum from MCPIP1$^{-/-}$ mice compared to that from MCPIP1$^{+/+}$ mice. Moreover, the mRNA levels for MD2, TLR4, CD14 and IL-6 were significantly increased in spleens from MCPIP1$^{-/-}$ compared to MCPIP1$^{+/+}$ mice (Fig.5b). No significant differences were observed in mRNA levels for TNFα, IL-1β, MCP-1, and iNOS in spleens from both genotypes, suggesting other sources may contribute the expression levels of these inflammatory cytokines. Consistent with the results above, the mRNA levels for many T cell cytokines including IFN-γ, IL-4, IL-5, IL-13, and IL-17 were markedly elevated in MCPIP1$^{-/-}$ compared to MCPIP1$^{+/+}$ mice (Fig. 5c). However, the expression levels of T-bet, GATA3 and RORγ were not changed, suggesting that MCPIP1 may directly regulate the mRNA degradation of IFN-γ, IL-4 and IL-17, but not their transcription. Among the B cell markers, the expression of marker of B cells progenitors, c-Kit, was up-regulated in MCPIP1$^{-/-}$ spleens, however, the expression of transcription factors for B cells development, EBF-1 and Pax5, was down-regulated in MCPIP1 deficient mice (Fig.5d). Interestingly, the expression of both Zc3h12b and Zc3h12c, but not Zc3h12d were compensatory increased in the spleen from MCPIP1$^{-/-}$ mice (Fig.5e). Taken together, these results further demonstrated that the fatal inflammatory syndrome in MCPIP1−/− mice was associated with an abnormal response of both innate and adaptive immune cells.

Antibiotic-treatment improves the life-span and inflammatory syndrome of MCPIP1-deficient mice

The indigenous microbiota of mucosal surfaces, particularly the intestinal microflora, accounts for a substantial proportion of the stimulus to our innate and adaptive immune systems[12, 13]. To test whether the indigenous microbiota contributed to the development of inflammatory phenotypes of MCPIP1-deficient mice, we treated MCPIP1 deficient and wild type mice from birth to 10 weeks with a combination of oral antibiotics that would greatly deplete the microflora of the intestine and other mucosal surfaces. As shown in Fig.6a, the survival rate of MCPIP1-deficient mice was significantly improved at 10 weeks by antibiotic-treatment; 80% of untreated MCPIP1$^{-/-}$ died, whereas only 33% of antibiotic MCPIP1$^{-/-}$ died by 10 weeks of age. Spleens from antibiotic-treated MCPIP1-deficient mice were much smaller than those from untreated MCPIP1-deficient mice (Fig. 6b). Furthermore, the mRNA expression levels encoding inflammatory cytokines such as IFN-γ,

IL-13 and IL-17, but not IL-6, were significantly decreased in speens from antibiotic-treated MCPIP1-deficient mice compared to untreated mice (Fig.6c).

Discussion

The key findings of the current study are that: 1) primary and secondary lymphoid organs of MCPIP1 deficient mice had signficant architectural abnormalities, and these abnormalities progressed with age; 2) MCPIP1-deficient mice spontanously developed profound, age-dependent, systemic inflammatory responses that involved both innate and adaptive immunity, as evidenced by marked infiltration of neutrophils, lymphocytes and macrophages into the lungs and liver, and by increased deposition of IgG and IgM in spleen, skin and lungs; 3) overall cellular composition of the spleen was markedly affected by MCPIP1 deficiency, as evidenced by greatly decrease in the numbers of B cells, marked increase in the numbers of neutrophils, slight decreases in T cells, and an increase in the proportion of the B cell lineage that had differentiated into plasma cells; 4) abnormal T cell populations in the spleen of MCPIP1 deficient mice that demonstrated enhanced immune activation; 5) protein and mRNA levels for numerous markers of innate and adaptive immunity were elevated in the sera and spleens from MCPIP1 deficient mice. Taken together, these results suggest that MCPIP1 deficient mice developed a lupus-like pathological changes except no glomerulonephritis.

The findings here support our original report that MCPIP1 is a negative regulator of inflammatory activation of macrophages[4] and extend our subsequent observations of the spontaneous, fatal, inflammatory disease that develops in MCPIP1-deficient mice[8]. In a report from Akira's group, Zc3h12a-deficient mice generated with a mixed C57BL/6 and 129/svj background showed a phenotype similar to our mouse line[9], suggesting that MCPIP1/Zc3h12a is essential to control inflammatory response and immune homeostasis. In addition, the phenotypes developed in MCPIP1-deficient mice share many similarities with mice deficient in TTP, roquin, TANK and TIPE2, etc.[14–17], suggesting that immune homeostasis is maintained by multiple negative regulators that could not compensate for each other. For example, the phenotypes of MCPIP1 deficient mice are resembled with the sanroque homozygous mice including enlarged spleen and lymph nodes, anemia, hepatitis, autoantibody production and accumulation of IgG-containing immnue complexes[15]. However, MCPIP1-deficenct mice did not show marked proliferative glomerolonephritis as the sanroque mice and MCPIP1-deficient mice showed obvious abnormalities in the innate arm that sanroque mice did not show. In addition, MCPIP1-deficient mice showed many phenotypes that resembled with TTP-knockout mice such as inflammatory arthritis, dermatitis, cachexia and autoimmunity[14]. In TTP-knockout mice, the phnotypes can be largely attributed to the incresed production of TNFα, whereas MCPIP1-deficient mice showed profound changes of many inflammatiory cytokines. In a recent report, myloid-specific TTP knockout mice showed extremely sensitive to LPS-induced septic shock[18], which is very similar to MCPIP1-deficent mice[10]. Considering roquin (sanroque), TTP (zfp36) and MCPIP1 (Zc3h12a) are all CCCH-zinc finger containing proteins, they may share some similar role and mechanisms in maintaing immune homeostasis.

Under physiological conditions, the commensal microbiota of mucosal surfaces represents the largest source of ligands for toll-like receptors, which serve as the principle sensors of the innate immune system. It has also been reported that TLR signaling by this commensal microbiota contributes to the pathogenesis of autoimmune diseases[12, 13]. To test whether commensal microbiota contributed to the pathogenesis of inflammatory disease in MCPIP1-deficient mice, we treated these mice for 10 weeks with a combination of antibiotics (ampicillin, neomycin, vancomycin, and metronidazole) that would have a collective broad spectrum of antibacterial activity and would be expected to eradicate much of commensal microbiota from the intestine and other mucosal surfaces. Importantly, treatment of MCPIP1 deficient mice with antibiotics reduced abnormalities observed in spleens, increased survival, and decreased mRNA levels for inflammatory cytokines. Consequently, this series of experiments clearly supported the conclusion that commensal microbiota contributed to development of the inflammatory and immune disorders developing in MCPIP1 deficient mice.

The molecular mechanisms underlying the pathological changes in MCPIP1-deficient mice are still not completely understood. The initial report[3] that MCPIP1 may be a transcription factor is not supported by following stuides . Emerging data indicated that MCPIP1 is a novel RNase, which may selectively target mRNA of some inflammatory cytokines such as IL-6, IL-1β, IL-2 and IL-12p40 for degradation[9, 19–21]. However, how MCPIP1 selectively target specific substrates is not clear. We recently observed that MCPIP1 forms granule-like structure in cytosol and is associated with the key components of RNA-induced silencing complex, such as Argnaute 2 and GW-182 (ref. 22). These data suggest that MCPIP1 may cooperate with miRNA effector pathway to silence the expression of specific inflammatory mRNAs. The previous work from us and others also suggests that MCPIP1 can inhibit inflammatory signaling especially JNK and NF-κB signal pathways[8,23,24]. Taken together, these results suggest that MCPIP1 may function as a multifunctional molecule that down-regulates inflammatory and immue responses through multiple mechanisms.

Methods

Mice

MCPIP1-deficient ($MCPIP1^{-/-}$) mice and their wild-type ($MCPIP1^{+/+}$) littermates on a C57BL/6 background were generated as described previously[8] and housed in the Laboratory Research Animal Center at the University of Missouri Kansas City. All mice were maintained in sterilized filter-top cages and fed autoclaved food and water under specific pathogen-free conditions. Both male and female mice used were between the ages of 6 and 12 weeks, unless indicated otherwise. Experimental procedures were approved by the Animal Care and Use Committee of University of Missouri Kansas City.

Histological Analyses

Tissue samples were fixed in 10% neutral buffered formalin for 1 day, subsequently routinely processed, and embedded in paraffin. Sections of 5 μm thickness were stained with hematoxylin and eosin (H&E). Slides were interpreted by a board-certified pathologist blinded to the genotypes of the specimens.

Immunohistochemistry and Immunofluorescence

5-μm sections of paraffin-embedded material were used for the immunologic staining. After rehydration, endogenous peroxidase was quenched by incubation of the sections in 0.3% H_2O_2 diluted in methanol for 30 minutes. Thereafter, antigen retrieval was performed using either citrate (pH 6.0) or EDTA (pH 8.0) for 15 minutes in the autoclave. After cooling, the slides were rinsed with phosphate-buffered saline (PBS) containing 0.5% Triton X-100 (5 minutes), followed by PBS only (3 × 5 minutes). After pre-incubation with normal donkey serum or normal goat serum, antibodies against CD45 and F4/80 (ABcam), DyLight 488 anti-mouse IgM, and DyLight 594 anti-mouse IgG (Vector Labs), were used for the analysis. CD45 (marker of B cells) and F4/80 (marker of macrophages) were detected with secondary antibody conjugated to horseradish peroxidase, followed by the addition of a chromogen substrate. DyLight 488 anti-mouse IgM and DyLight 594 anti-mouse IgG were used for immunofluorescence. Sections were counterstained with hematoxylin and DAPI (4′, 6′-diamidino-2-phenylindole) for immunohistochemistry and immunofluorescence, respectively.

Flow Cytometry

Mouse spleen cells were collected and the red blood cells were lysed with BD lysing buffer (BD Biosciences). The non-lysed cells were further stained with antibodies against surface markers to distinguish subpopulations. For cytokine expression assay, the cells were first cultured with RPMI1640 medium containing 10% FBS (Hyclone) for 5 hours in the presence of 1 μg/ml BFA, 1 μg/ml ionomycin and 50 ng/ml PMA (all from Sigmaaldrich) and then labelled. All of the intracellular labelling was performed after the surface marker staining with Foxp3 staining buffer set (eBioscience) following the manufacturer's instructions. The flow-cytometry antibodies used include anti-CD3ε (PerCP-Cy5.5), anti-B220 (PE-Cy7), anti-CD4 (APC), anti-CD8 (FITC), anti-CD62L (PE), anti-IFN-γ (PE), anti-IL-4 (PE), anti-IL-17 (PE), anti-Foxp3 (PE), anti-CD11b (PE), anti-CD115 (PerCP-eFluor710), anti-Ly-6C (APC) (all above from eBioscience), anti-CD138 (APC) and anti-Ly-6G (FITC) (both from BD Biosciences) antibodies. Data analysis was performed using the CellQuest software.

ELISA and QPCR

ELISA was performed by using Bio-Plex Pro Mouse Cytokine 23-plex Assay according to the manufacturer's instruction. Real-time polymerase chain reactions (PCR) were performed using SYBR Green PCR master mix (Applied Biosystems, Foster City, CA) on a StepOnePlus real-time PCR system (Applied Biosystems) following standard procedures. Briefly, single-stranded cDNA was synthesized from 1 μg of total RNA using High Capacity cDNA Reverse Transcription Kit (Applied Biosystems). For PCR reactions, 1 μl of DNA template, 0.3 μl of forward and reverse primers (10 μmol/L each), 10 μl of SYBR Green PCR Master Mix, and 8.4 μl of water were added to a final volume of 20 μl. Thermal cycling was performed as follows: 95°C for 3 minutes as initial denaturing, followed by 40 cycles of 94°C for 30 seconds, 60°C for 30 seconds, and a final extension at 72°C for 2 minutes. Threshold cycles (C_T values) were determined using the StepOne software (Applied Biosystems). The sequence of the primers used for the PCR will be sent per request. Real-

time PCR results were normalized using β-actin as an internal control. Relative mRNA levels were calculated from the C_T values for each sample.

Antibiotic Treatment

Both MCPIP1-deficient mice and their wild-type littermates received untreated water or treated water containing ampicillin (1 g/L), neomycin (1 g/L), vancomycin (0.5 g/L) and metronidazole (1 g/L) from birth to 10 weeks. The body weight and survival rate were recorded. At 10 weeks, surviving mice were sacrificed and the spleens were weighed and photographed. Cytokine expression in the spleen was measured by QPCR.

Statistics

Data were expressed as mean±SD. For comparison between two groups, the unpaired Student's test was used. For multiple comparisons, analysis of variance followed by unpaired Student's test was used. A value of $p<0.05$ was considered significant.

Supplementary Material

Refer to Web version on PubMed Central for supplementary material.

Acknowledgments

We thank Ms. Ruth E. Morgan for helping with the experiments of flow cytometry. Flow cytometry was performed in the Children's Mercy Hospital and Clinics Core Clinical and Research Flow Cytometry Laboratory. This work was partially supported by National Institute of Health Grants (HL098794 to M.F., HL097218 and HL076206 to G.L., HL068878 and HL089544 to Y.E.C.). Y.E.C. is an Established Investigator of the American Heart Association (0840025N).

Abbreviations

MCPIP1	MCP-induced protein 1
TNF	tumor necrosis factor
NF-κB	nuclear factor-κB
IL-1β	interleukin 1β
MCP-1	monocyte chemotactic protein-1
LPS	lipopolysaccharide
TLR	toll-like receptor
IFN	interferon
TRAF	TNF receptor associate factor

References

1. Van Parijs L, Abbas AK. Homeostasis and self-tolerance in the immune system: turning lymphocytes off. Science. 1998; 280:243–248. [PubMed: 9535647]
2. Stockinger B, Kassiotis G, Bourgeois C. Homeostasis and T cell regulation. Curr Opin Immunol. 2004; 16:775–779. [PubMed: 15511672]

3. Zhou L, Azfer A, Niu J, Graham S, Choudhury M, Adamski FM, et al. Monocyte chemoattractant protein-1 induces a novel transcription factor that causes cardiac myocyte apoptosis and ventricular dysfunction. Circ Res. 2006; 98:1177–1185. [PubMed: 16574901]
4. Liang J, Wang J, Azfer A, Song W, Tromp G, Kolattukudy PE, et al. A novel CCCH-zinc finger protein family regulates proinflammatory activation of macrophages. J Biol Chem. 2008; 283:6337–6346. [PubMed: 18178554]
5. Liang J, Song W, Tromp G, Kolattukudy PE, Fu M. Genome-wide survey and expression profiling of CCCH-zinc finger family reveals a functional module in macrophage activation. PLoS One. 2008; 3:e2880. [PubMed: 18682727]
6. Skalniak L, Mizgalska D, Zarebski A, Wyrzykowska P, Koj A, Jura J. Regulatory feedback loop between NF-kappaB and MCP-1-induced protein 1 RNase. FEBS J. 2009; 276:5892–5905. [PubMed: 19747262]
7. Kasza A, Wyrzykowska P, Horwacik I, Tymoszuk P, Mizgalska D, Palmer K, et al. Transcription factors Elk-1 and SRF are engaged in IL1-dependent regulation of ZC3H12A expression. BMC Mol Biol. 2010; 11:14. [PubMed: 20137095]
8. Liang J, Saad Y, Lei T, Wang J, Qi D, Yang Q, et al. MCP-induced protein 1 deubiquitinates TRAF proteins and negatively regulates JNK and NF-kappaB signaling. J Exp Med. 2010; 207:2959–2973. [PubMed: 21115689]
9. Matsushita K, Takeuchi O, Standley DM, Kumagai Y, Kawagoe T, Miyake T, et al. Zc3h12a is an RNase essential for controlling immune responses by regulating mRNA decay. Nature. 2009; 458:1185–1190. [PubMed: 19322177]
10. Huang S, Miao R, Zhou Z, Wang T, Liu J, Liu G, et al. MCPIP1 negatively regulates Toll-like receptor 4 signaling and protects mice from LPS-induced septic shock. Cell Signal. 2013 (in press).
11. Lin RJ, Chien HL, Lin SY, Chang BL, Yu HP, Tang WC, et al. MCPIP1 ribonuclease exhibits broad-spectrum antiviral effects through viral RNA binding and degradation. Nucleic Acids Res. 2013 (in press).
12. Saleh M, Elson CO. Experimental inflammatory bowel disease: insights into the host-microbiota dialog. Immunity. 2011; 34:293–302. [PubMed: 21435584]
13. Feng T, Elson CO. Adaptive immunity in the host-microbiota dialog. Mucosal Immunol. 2011; 4:15–21. [PubMed: 20944557]
14. Taylor GA, Carballo E, Lee DM, Lai WS, Thompson MJ, Patel DD, et al. A pathogenetic role for TNFalpha in the syndrome of cachexia, arthritis, and autoimmunity resulting from tristetraprolin (TTP) deficiency. Immunity. 1996; 4:445–454. [PubMed: 8630730]
15. Vinuesa CG, Cook MC, Angelucci C, Athanasopoulos V, Rui L, Hill KM, et al. A RING-type ubiquitin ligase family member required to repress follicular helper T cells and autoimmunity. Nature. 2005; 435:452–458. [PubMed: 15917799]
16. Kawagoe T, Takeuchi O, Takabatake Y, Kato H, Isaka Y, Tsujimura T, et al. TANK is a negative regulator of Toll-like receptor signaling and is critical for the prevention of autoimmune nephritis. Nat Immunol. 2009; 10:965–972. [PubMed: 19668221]
17. Sun H, Gong S, Carmody RJ, Hilliard A, Li L, Sun J, et al. TIPE2, a negative regulator of innate and adaptive immunity that maintains immune homeostasis. Cell. 2008; 133:415–426. [PubMed: 18455983]
18. Qiu LQ, Stumpo DJ, Blackshear PJ. Myeloid-specific tristetraprolin deficiency in mice results in extreme lipopolysaccharide sensitivity in an otherwise minimal phenotype. J Immunol. 2012; 188:5150–5159. [PubMed: 22491258]
19. Mizgalska D, Wegrzyn P, Murzyn K, Kasza A, Koj A, Jura J, et al. Interleukin-1-inducible MCPIP protein has structural and functional properties of RNase and participates in degradation of IL-1beta mRNA. FEBS J. 2009; 276:7386–7399. [PubMed: 19909337]
20. Xu J, Peng W, Sun Y, Wang X, Xu Y, Li X, et al. Structural study of MCPIP1 N-terminal conserved domain reveals a PIN-like RNase. Nucleic Acids Res. 2012; 40:6957–6965. [PubMed: 22561375]
21. Li M, Cao W, Liu H, Zhang W, Liu X, Cai Z, et al. MCPIP1 down-regulates IL-2 expression through an ARE-independent pathway. PLoS One. 2012; 7:e49841. [PubMed: 23185455]

22. Qi D, Huang S, Miao R, She ZG, Quinn T, Chang Y, et al. Monocyte chemotactic protein-induced protein 1 (MCPIP1) suppresses stress granule formation and determines apoptosis under stress. J Biol Chem. 2011; 286:41692–41700. [PubMed: 21971051]

23. Liang J, Wang J, Saad Y, Warble L, Becerra E, Kolattukudy PE. Participation of MCP-induced protein 1 in lipopolysaccharide preconditioning-induced ischemic stroke tolerance by regulating the expression of proinflammatory cytokines. J Neuroinflammation. 2011; 8:182. [PubMed: 22196138]

24. Niu J, Wang K, Graham S, Azfer A, Kolattukudy PE. MCP-1-induced protein attenuates endotoxin-induced myocardial dysfunction by suppressing cardiac NF-κB activation via inhibition of IκB kinase activation. J Mol Cell Cardiol. 2011; 51:177–186. [PubMed: 21616078]

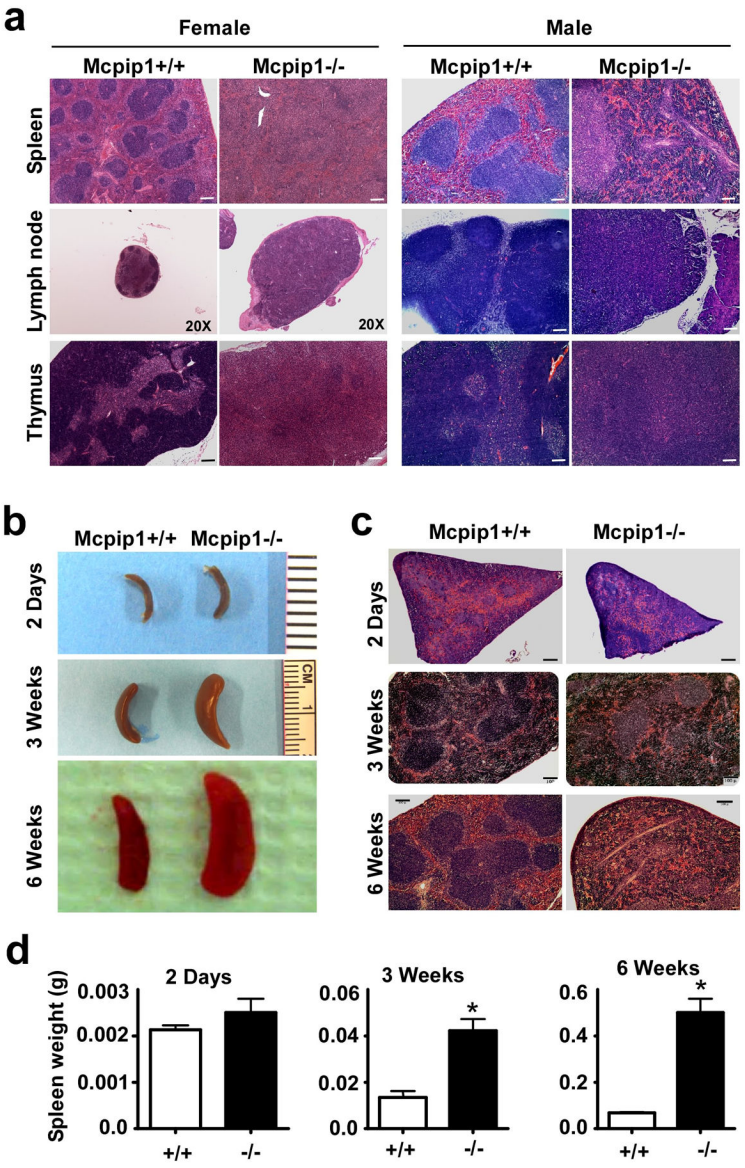

Figure 1. Disorganization of lympoid organs from MCPIP1$^{-/-}$ mice

a) H&E staining of formalin-fixed spleen, lymph node and thymus sections from both male and female MCPIP1$^{-/-}$ mice and wild-type littermates (MCPIP1$^{+/+}$) at the age of 8–10 weeks. Magnitude is 100× except indicated. Bar=100μm. **b)** Gross morphology of the spleen from MCPIP1$^{+/+}$ and MCPIP1$^{-/-}$ mice at the indicated age. **c)** H&E staining of the spleen from MCPIP1$^{+/+}$ and MCPIP1$^{-/-}$ mice at the indicated age. Bar=100μm. **d)** The spleen weight from MCPIP1$^{+/+}$ and MCPIP1$^{-/-}$ mice at the indicated age. N=3. *P<0.05 vs wild-type group.

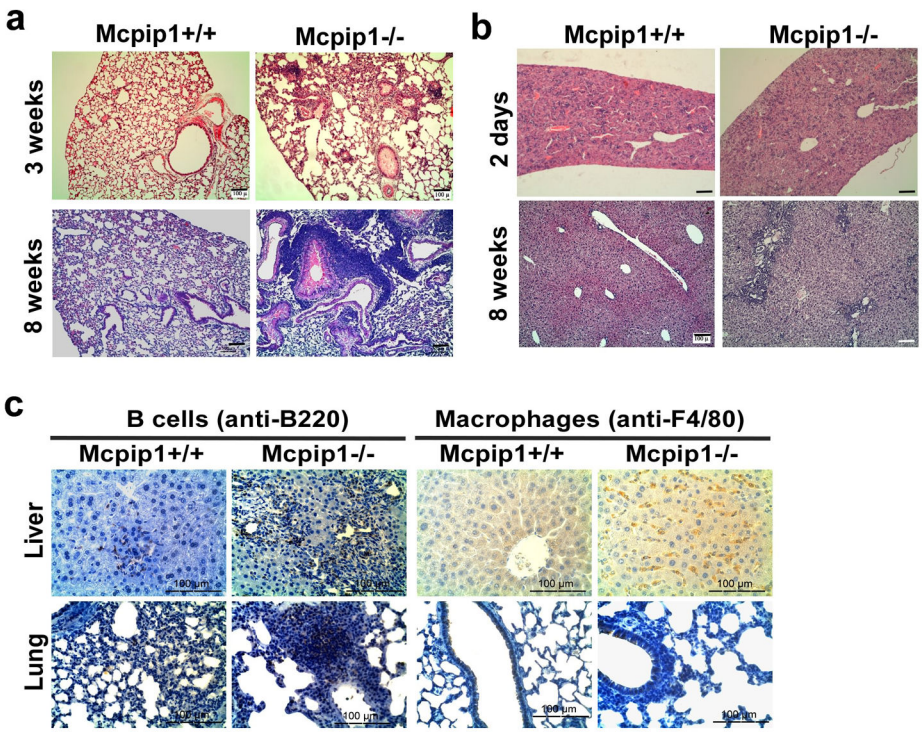

Figure 2. Development of multi-organ inflammation in MCPIP1$^{-/-}$ mice

a) H&E staining of formalin-fixed lung sections from MCPIP1$^{-/-}$ mice and wild-type littermates at the indicated age. **b)** H&E staining of formalin-fixed liver sections from MCPIP1$^{-/-}$ mice and wild-type littermates at the indicated age. **c)** Immunohistochemical staining of formalin fixed liver and lung sections from MCPIP1 null mice and wild-type littermates at the age of 8 weeks with B cell marker (anti-B220) and macrophage marker (anti-F4/80).

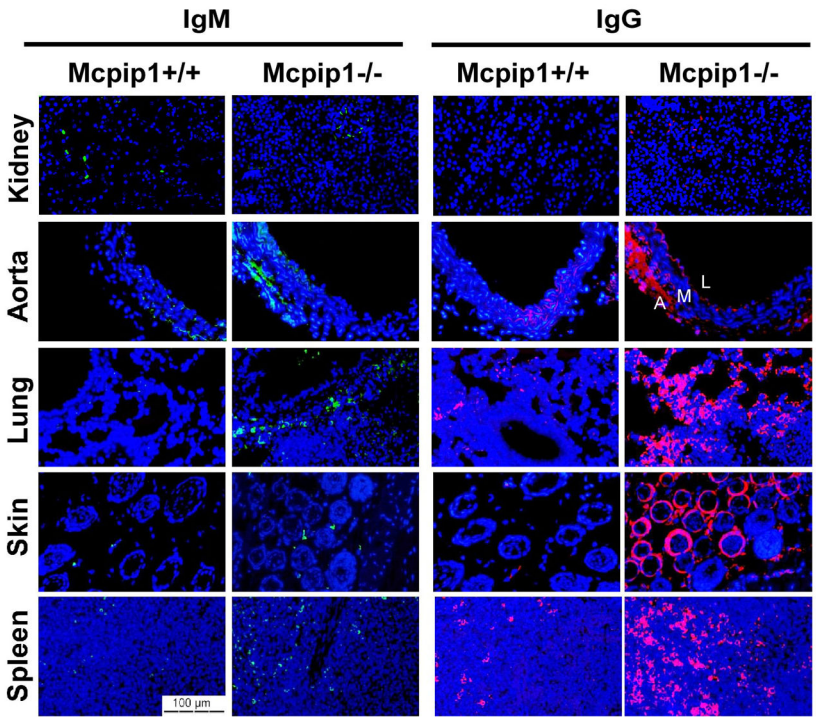

Figure 3. Immunoglobulin accumulation in in MCPIP1$^{-/-}$ mice

Immunofluoresence staining of formalin-fixed kidney, aorta, lung, skin and spleen sections from MCPIP1$^{-/-}$ mice and wild-type littermates at the age 8 weeks with anti-IgM and anti-IgG. The layers of aorta have been marked as “A” (adventitial), “M” (media layer) and “L” (lumen).

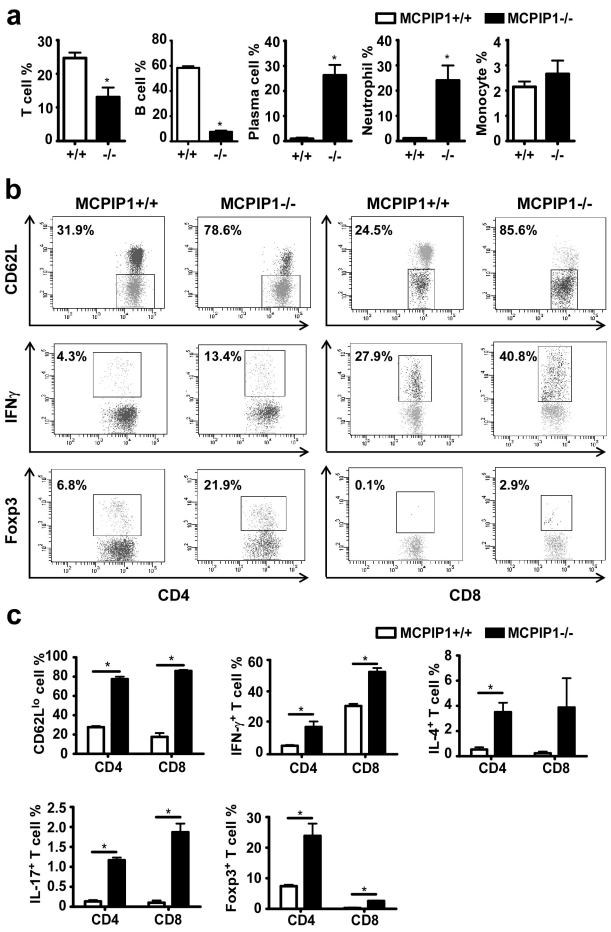

Figure 4. Immune cell abnormalities in MCPIP1-deficient spleens

Single-cell suspensions of spleens from 6-week-old wild-type and MCPIP1$^{-/-}$ mice were counted and stained for flow cytometric analysis. **a)** The percentage of total T cells, B cells, neutrophils and monocytes in total nucleared cells, and the percentage of B cells that had differentiated to plasma cells were reported as mean±SD, n=3. *P<0.01 vs wild-type mice. **b)** Flow cytometry plots for CD62L, IFNγ, and Foxp3 in CD4$^+$ and CD8$^+$ cells. **c)** The percentage of subtypes of T cells in both CD4+ and CD8+ T cell populations were reported as mean±SD, n=3. *P<0.01 vs wild-type mice.

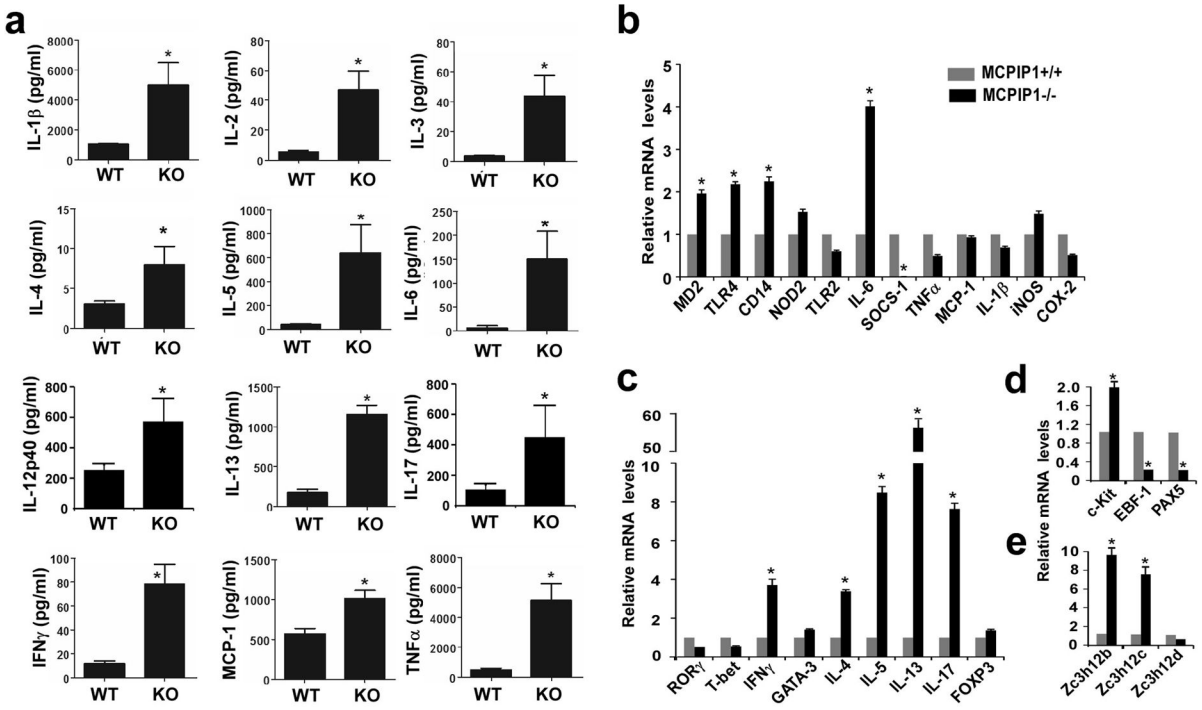

Figure 5. Expression of proinflammatory cytokines, chemokines, and other markers of inflammation from MCPIP1$^{-/-}$ and MCPIP1$^{+/+}$ mice

a) ELISA analysis of serum levels of proinflammatory cytokines, chemokines, and other markers of inflammation of MCPIP1-deficient mice (KO) and their wild-type littermates (WT) at the age of 6–8 weeks (n=3 per genotype). Data are presented as mean±SD, n=3. *P<0.01 vs wild-type mice. **b–d)** QPCR analysis of mRNA levels of proinflammatory cytokines, chemokines, and other markers of inflammation in spleens of MCPIP1-deficient mice and their wild-type littermates at the age of 6–8 weeks (n=3 per genotype). Data are presented as mean±SD, n=3. *P<0.01 vs wild-type mice. **e)** QPCR analysis of the mRNA levels of Zc3h12b, Zc3h12c and Zc3h12d in the spleens of MCPIP1-deficient mice and their wild-type littermates at the age of 6–8 weeks (n=3 per genotype).

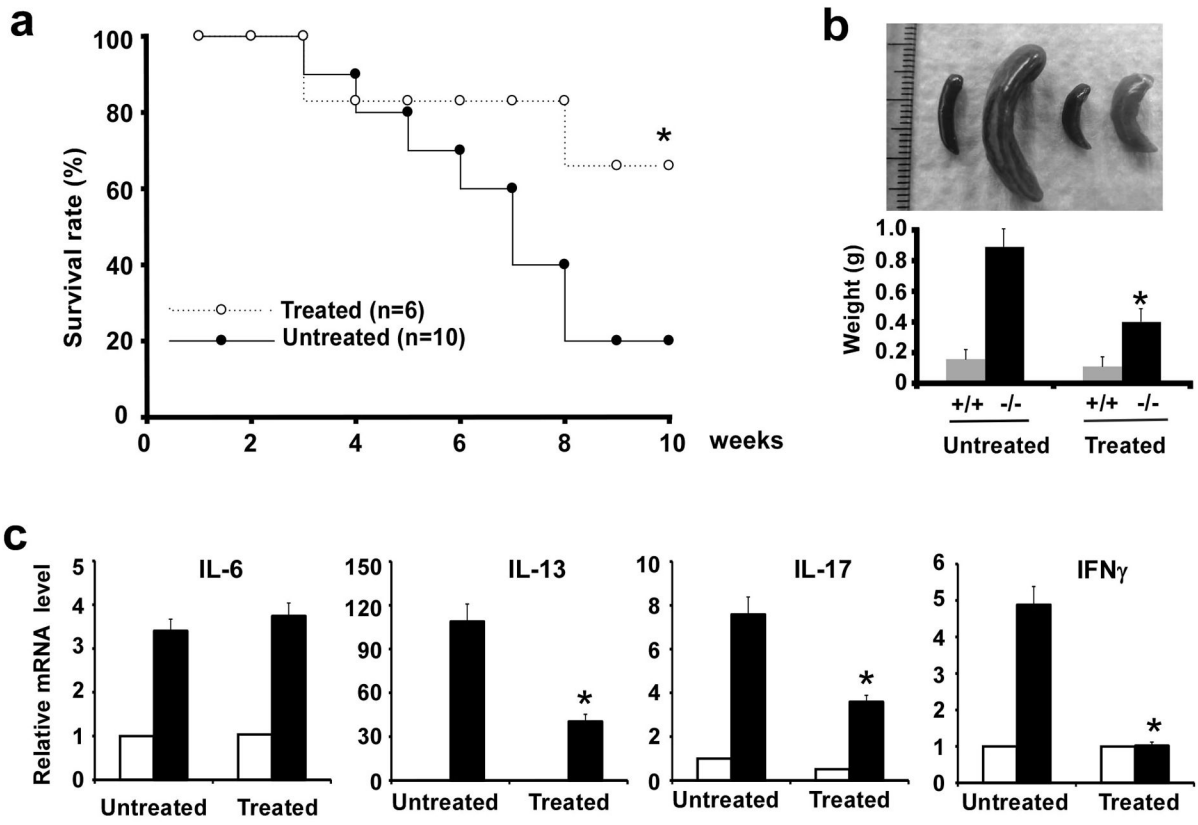

Figure 6. Antibiotic treatment improved the life-span and inflammatory syndrome of MCPIP1$^{-/-}$ mice

a) MCPIP1-deficient mice were treated orally with the drinking water containing ampicillin (1 g/L), neomycin (1 g/L), vancomycin (0.5 g/L) and metronidazole (1 g/L) (n=6) or normal drinking water (n=10) from birth to 10-weeks of age. The survival rates from both groups were recorded and plotted. *P<0.05. **b)** Representive gross morphology and weight of spleens from antibiotic treated and untreated MCPIP1$^{+/+}$ and MCPIP1$^{-/-}$ mice. *P<0.05, n=3. **c)** QPCR analysis of mRNA levels of proinflammatory cytokines in the spleens from antibiotic treated and untreated MCPIP1$^{+/+}$ and MCPIP1$^{-/-}$ mice. Data were represented as mean±SD, n=3. *P<0.01 vs untreated MCPIP1$^{-/-}$ mice. The solid bar indicates MCPIP1$^{-/-}$ mice and the open bar indicates wild type mice.